Chapter 1

Introduction

Optical fibers have revolutionized telecommunication. Much of the success of optical fiber lies in its near-ideal properties: low transmission loss, high optical damage threshold, and low optical nonlinearity. The combination of these properties has enabled long-distance communication to become a reality. At the same time, the long lengths enabled the optical power to interact with the small nonlinearity to give rise to the phenomenon of optical solitons, overcoming the limit imposed by linear dispersion. The market for optical fiber continues to grow, despite the fact that major trunk routes and metropolitan areas have already seen a large deployment of fiber. The next stage in the field of communication is the mass delivery of integrated services, such as home banking, shopping, Internet services, and entertainment using video-on-demand. Although the bandwidth available on single mode fiber should meet the ever-increasing demand for information capacity, architectures for future networks need to exploit technologies which have the potential of driving down cost to make services economically viable. Optical fiber will have to compete with other transport media such as radio, copper cable, and satellite. Short-term economics and long-term evolutionary potential will determine the type of technology likely to succeed in the provision of these services. But it is clear that optical fibers will play a crucial role in communication systems of the future. The technological advances made in the field of photosensitive optical fibers are relatively recent; however, an increasing number of fiber devices based on this technology are getting nearer to the market place. It is believed that they will provide options to the network designer that should influence, for example, the deployment of wavelength-division-multiplexed (WDM) systems, channel selection, and deployment of transmitters in the upstream path in a network, and should make routing viable. The fascinating technology of photosensitive fiber is based on the principle of a simple in-line all-fiber optical filter, with a vast number of applications to its credit.

1.1 Historical perspective

Photosensitivity of optical fiber was discovered at the Canadian Communication Research Center in 1978 by Ken Hill *et al.* [1] during experiments using germania-doped silica fiber and visible argon ion laser radiation. It was noted that as a function of time, light launched into the fiber was increasingly reflected. This was recognized to be due to a refractive index grating written into the core of the optical fiber as a result of a standing wave intensity pattern formed by the 4% back reflection from the far end of the fiber and forward-propagating light. The refractive index grating grew in concert with the increase in reflection, which in turn increased the intensity of the standing wave pattern. The periodic refractive index variation in a meter or so of fiber was a Bragg grating with a bandwidth of around 200 MHz. But the importance of the discovery in future applications was recognized even at that time. This curious phenomenon remained the preserve of a few researchers for nearly a decade [2,3]. The primary reason for this is believed to be the difficulty in setting up the original experiments, and also because it was thought that the observations were confined to the one "magic" fiber at CRC. Further, the writing wavelength determined the spectral region of the reflection grating, limited to the visible part of the spectrum.

Researchers were already experimenting and studying the even more bizarre phenomenon of second-harmonic generation in optical fibers made of germania-doped silica, a material that has a zero second-order nonlinear coefficient responsible for second-harmonic generation. The observation was quite distinct from another nonlinear phenomenon of sum-frequency generation reported earlier by Ohmori and Sasaki [4] and Hill *et al.* [5], which were also curious. Ulf Österberg and Walter Margulis [6] found that ML-QS infrared radiation could "condition" a germania doped-silica fiber after long exposure such that second-harmonic radiation grew (as did Ken Hill's reflection grating) to nearly 5% efficiency and was soon identified to be a grating formed by a nonlinear process [7,8]. Julian

Stone's [9] observation that virtually any germania-doped silica fiber demonstrated a sensitivity to argon laser radiation reopened activity in the field of fiber gratings [10,11] and for determining possible links between the two photosensitive effects. Bures *et al.* [12] had pointed out the two-photon absorption nature of the phenomenon from the fundamental radiation at 488 nm.

The major breakthrough came with the report on holographic writing of gratings using single-photon absorption at 244 nm by Gerry Meltz *et al.* [13]. They demonstrated reflection gratings in the visible part of the spectrum (571–600 nm) using two interfering beams external to the fiber. The scheme provided the much-needed degree of freedom to shift the Bragg condition to longer and more useful wavelengths, predominantly dependent on the angle between the interfering beams. This principle was extended to fabricate reflection gratings at 1530 nm, a wavelength of interest in telecommunications, also allowing the demonstration of the first fiber laser operating from the reflection of the photosensitive fiber grating [14]. The UV-induced index change in untreated optical fibers was $\sim 10^{-4}$. Since then, several developments have taken place that have pushed the index change in optical fibers up a hundredfold, making it possible to create efficient reflectors only a hundred wavelengths long. Lemaire and coworkers [15] showed that the loading of optical fiber with molecular hydrogen photosensitized even standard telecommunication fiber to the extent that gratings with very large refractive index modulation could be written.

Pure fused silica has shown yet another facet of its curious properties. It was reported by Brueck *et al.* [16] that at 350°C, a voltage of about 5 kV applied across a sheet of silica, a millimeter thick, for 30 minutes resulted in a permanently induced second-order nonlinearity of ~1 pm/V. Although poling of optical fibers had been reported earlier using electric fields and blue-light and UV radiation [17–19], Wong *et al.* [20] demonstrated that poling a fiber while writing a grating with UV light resulted in an enhanced electro-optic coefficient. The strength of the UV-written grating could be subsequently modulated by the application of an electric field. More recently, Fujiwara *et al.* reported a similar photoassisted poling of bulk germanium-doped silica glass [21]. The silica–germanium system will no doubt produce further surprises.

All these photosensitive processes are linked in some ways but can also differ dramatically in their microscopic detail. The physics of the effect continues to be debated, although the presence of defects plays a central role in more than one way. The field remains an active area for research.

1.2 Materials for glass fibers

Optical fiber for communications has evolved from early predictions of lowest loss in the region of a few decibels per kilometer to a final achieved value of only 0.2 dB km^{-1}. The reason for the low optical loss is several fortuitous material properties. The bandgap of fused silica lies at around 9 eV [22], while the infrared vibrational resonances produce an edge at a wavelength of around 2 microns. Rayleigh scatter is the dominant loss mechanism with its characteristic λ^{-4} dependence in glass fibers indicating a near perfect homogeneity of the material [23]. The refractive index profile of an optical fiber is shown in Fig. 1.1. The core region has a higher refractive index than the surrounding cladding material, which is usually made of silica. Light is therefore trapped in the core by total internal reflection at the core–cladding boundaries and is able to travel tens of kilometers with little attenuation in the 1550-nm wavelength region. One

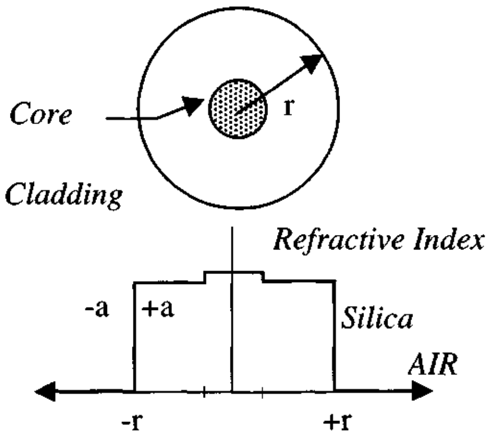

Figure 1.1: Cross-section of an optical fiber with the corresponding refractive index profile. Typically, the core-to-cladding refractive index difference for single-mode telecommunications fiber at a wavelength of 1.5 μm is ~4.5×10^{-3} with a core radius of 4 μm.

of the commonly used core dopants, germanium, belongs to Group IVA, as does silicon and replaces the silicon atom within the tetrahedron, coordinated with four oxygen atoms. Pure germania has a band edge at around 185 nm [24]. Apart from these pure material contributions, which constitute a fundamental limit to the attenuation characteristics of the waveguide, there may be significant absorption loss from the presence of impurities. The OH^- ion has IR absorptions at wavelengths of 1.37, 0.95, and 0.725 μm [25], overtones of a stretching-mode vibration at a fundamental wavelength of 2.27 μm. Defect states within the ultraviolet and visible wavelength band of 190–600 nm [26] also contribute to increased absorption. The properties of some of these defects will be discussed in Chapter 2.

The presence of phosphorus as P_2O_5 in silica, even in small quantities (~0.1%), reduces the glass melting point considerably, allowing easier fabrication of the fiber. Phosphorus is also used in fibers doped with rare earth compounds such as Yb and Er for fiber amplifiers and lasers. In high concentration rare earth ions tend to cluster in germanium-doped silicate glasses. Clustering causes ion–ion interaction, which reduces the excited state lifetimes [27]. Along with aluminum (Al_2O_3 as a codopant in silica) in the core, clustering is greatly reduced, enabling efficient amplifiers to be built. Phosphorus is also commonly used in planar silica on silicon waveguide fabrication, since the reduced processing temperature reduces the deformation of the substrate [28].

Fluorine and trivalent boron (as B_2O_3) are other dopants commonly used in germania-doped silica fiber. A major difference between germanium and fluorine/boron is that while the refractive index increases with increasing concentration of germanium, it decreases with boron/fluorine. With fluorine, only modest reductions in the refractive index are possible (~0.1%), whereas with boron large index reductions (>0.02) are possible. Boron also changes the topology of the glass, being trivalent. Boron and germanium together allow a low refractive index difference between the core and cladding to be maintained with large concentrations of both elements [29]. On the other hand, a depressed cladding fiber can be fabricated by incorporating boron in the cladding to substantially reduce the refractive index.

The density of the boron-doped glass may be altered considerably by annealing, by thermally cycling the glass, or by changing the fiber drawing temperature [30]. Boron-doped preforms exhibit high stress and shatter easily unless handled with care. The thermal history changes the density and stress in the glass, thereby altering the refractive index. The thermal expansion of boron–silica glass is $\sim 4 \times 10^{-6}$°C^{-1}, several times that of silica (7×10^{-7}°C^{-1}) [31]. Boron-doped silica glass is generally free of defects, with a much reduced melting temperature. Boron being a lighter atom, the vibrational contribution to the absorption loss extends deeper into the short wavelength region and increases the absorption loss in the 1500-nm window. Boron with germanium doping has been shown to be excellent for photosensitivity [29].

1.3 Origins of the refractive index of glass

The refractive index n of a dielectric may be expressed as the summation of the contribution of i oscillators of strength f_i each, as [32]

$$\frac{n^2 - 1}{n^2 + 2} = \frac{4\pi}{3} \frac{e^2}{m\varepsilon_0} \sum_i \frac{f_i}{\omega_i^2 - \omega^2 + i\Gamma_i \omega}, \tag{1.1.1}$$

where e and m are the charge and mass of the electron, respectively, ω_i is the resonance frequency, and Γ_i is a damping constant of the ith oscillator. Therefore, refractive index is a complex quantity, in which the real part contributes to the phase velocity of light (the propagation constant), while the sign of the imaginary part gives rise to either loss or gain. In silica optical fibers, far away from the resonances of the deep UV wavelength region, which contribute to the background refractive index, the loss is negligible at telecommunications wavelengths. However, the presence of defects or rare-earth ions can increase the absorption, even within in the transmission windows of 1.3 to 1.6 microns in silica optical fiber.

Γ_i can be neglected in low-loss optical fibers in the telecommunications transmission band, so that the real part, the refractive index, is [32]

$$n^2 = 1 + \sum_i \frac{A_i \lambda^2}{\lambda^2 - \lambda_i^2}. \tag{1.1.2}$$

With $i = 3$, we arrive at the well-known Sellmeier expression for the refractive index, and for silica (and pure germania), the λ_i ($i = 1 \rightarrow 3$) are the electronic resonances at 0.0684043 (0.0690) and 0.1162414 (0.1540) μm, and lattice vibration at 9.896161 (11.8419) μm. Their strengths A_i have been experimentally found to be 0.6961663 (0.8069), 0.4079426 (0.7182), and 0.8974794 (0.8542) [33,34], where the data in parentheses refers to GeO_2. The group index N is defined as

$$N = n - \lambda \frac{dn}{d\lambda}, \tag{1.1.3}$$

which determines the velocity at which a pulse travels in a fiber. These quantities are plotted in Fig. 1.2, calculated from Eqs. (1.1.2) and (1.1.3). We note that the refractive index of pure silica at 244 nm at 20°C is 1.51086. The data for germania-doped silica may be found by interpolation of the data for the molar concentration of both materials. Although this applies to the equilibrium state in bulk samples, they may be modified by the fiber fabrication process.

The change in the refractive index of the fiber at a wavelength λ may be calculated from the observed changes in the absorption spectrum in the ultraviolet using the Kramers–Kronig relationship [32,35],

$$\Delta n(\lambda) = \frac{1}{(2\pi)^2} \sum_i \int_{\lambda_2}^{\lambda_1} \frac{(\Delta\alpha_i(\lambda') \cdot \lambda^2)}{(\lambda^2 - \lambda'^2)} d\lambda', \tag{1.1.4}$$

where the summation is over discrete wavelength intervals around each of the i changes in measured absorption, α_i. Therefore, a source of photoinduced change in the absorption at $\lambda_1 \leq \lambda' \leq \lambda_2$ will change the refractive index at wavelength λ.

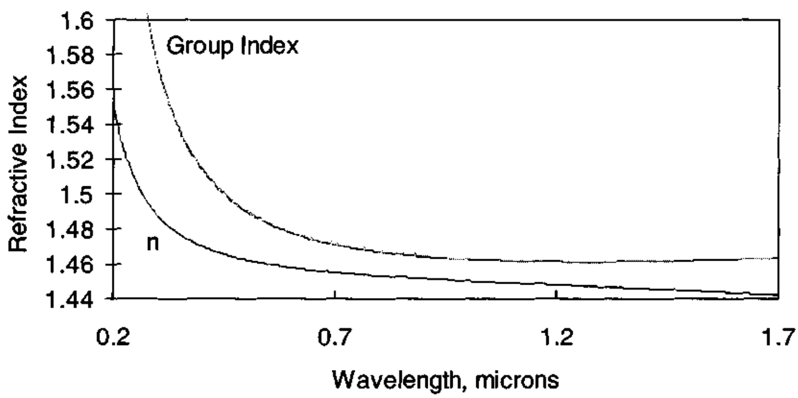

Figure 1.2: Refractive index n and the group index, N of pure silica at 20°C.

The refractive index of glass depends on the density of the material, so that a change in the volume through thermally induced relaxation of the glass will lead to a change Δn in the refractive index n as

$$\frac{\Delta n}{n} \approx \frac{\Delta V}{V} \approx \frac{3n}{2}\varepsilon, \tag{1.1.5}$$

where the volumetric change ΔV as a fraction of the original volume V is proportional to the fractional change ε in linear dimension of the glass.

We now have the fundamental components that may be used to relate changes in the glass to the refractive index after exposure to UV radiation.

Other interesting data on fused silica is its softening point at 2273°C, and the fact that it probably has the largest elastic limit of any material, ~17%, at liquid nitrogen temperatures [36].

1.4 Overview of chapters

The book begins with a simple introduction to the photorefractive effect as a comparison with photosensitive optical fibers in Chapter 2. The interest in electro-optic poled glasses is fueled from two directions: an interest in the physics of the phenomenon and its connection with photosensitive Bragg gratings, and as the practical need for devices that overcome many of the fabrication problems associated with crystalline electro-optic materials, of cutting, polishing, and in–out coupling. A fiber-compatible device is an ideal, which is unlikely to be abandoned. The fiber Bragg grating goes a long way in that direction. However interesting the subject of poled glasses and second-harmonic generation in glass optical fibers and nonlinear behavior of gratings, they are left for another time. With this connection left for the moment, we simply point to the defects, which are found to be in common with the process of harmonic generation, poling of glass, and Bragg gratings. The subject of defects alone is a vast spectroscopic minefield. Some of the prominent defects generally found in germania-doped fused silica that have a bearing on Bragg grating formation are touched upon. The nature and detection of the defects are introduced. This is followed by the process of photosensitizing optical fibers, including reduced germania, boron–germanium codoped fibers, Sn doping, and hydrogen loading. The different techniques and routes used to enhance the sensitivity of optical fibers, including that of rare-earth doped fibers are compared in a summary at the end of Chapter 2.

Chapter 3 is on fabrication of Bragg gratings. It deals with the principles of holographic, point-by-point replication and the technologies involved in the process: various arrangements of the Lloyd and mirror interferometers, phase-mask, along with the fabrication of different type of Bragg and long-period gratings, chirped gratings, and ultralong gratings. The attributes of some of the laser sources commonly used for fabrication are introduced in the concluding section of the chapter.

Chapter 4 begins with wave propagation in optical fibers, from the polarization response of a dielectric to coupled mode theory, and formulates the basic equations for calculating the response of uniform gratings. A section follows on the side-tap gratings, which have special applications as lossy filters. Antenna theory is used to arrive at a good approximation to the filter response for the design of optical filters. Long-period gratings and their design follow, as well as the physics of rocking filters. The last section deals with grating simulation. Here two methods for the simulation of gratings of arbitrary profile and chirp based on the transfer-matrix approach and Rouard's method of thin films are described.

Chapter 5 looks in detail at the different methods available for apodization of Bragg gratings and its effect on the transfer characteristics. These include the use of the phase mask, double exposure, stretching methods, moiré gratings, and novel schemes that use the coherence properties of lasers to self-apodize gratings.

Chapter 6 introduces the very large area of band-pass filtering to correct for the "errant" property of the Bragg grating: as the band-stop filter! We begin with the distributed-feedback (DFB) structure as the simplest transmission Bragg grating, followed by the multisection grating design for the multiple band-pass function, chirped grating DFB band-pass filters widening the gap to address the Fabry–Perot structure, and moving on to the superstructure grating. Other schemes include the Michelson-interferometer-based filter, Mach–Zehnder interferometer, properties, tolerances requirements for fabrication, and a new device based on the highly detuned interferometer, which allows multiple band-pass filters to be formed, using chirped and unchirped gratings. An important area in applications is the optical add–drop multiplexer (OADM), and different configurations of these are considered, along with their advantages and disadvantages. The special filter based on the in-coupler Bragg grating as a family of filters is presented. Simple equations are suggested for simulating the response of the Bragg reflection coupler. Rocking and mode-converting filters are also presented, along with the side-tap radiation mode and long period grating filter, as band-pass elements.

Chirped gratings have found a niche as dispersion compensators. Therefore, Chapter 7 is devoted to the application of chirped gratings, with a detailed look at the dispersive properties related to apodization and imperfect fabrication conditions on the group delay and reflectivity of gratings. Further, the effect of stitching is considered for the fabrication of long gratings, and the effect of cascading gratings is considered for systems applications. Systems simulations are used to predict the bit-error-rate performance of both apodized and unapodized gratings. Transmission results are also briefly reviewed.

The applications of gratings in semiconductor and fiber lasers can be found in Chapter 8. Here configurations of the external cavity fiber Bragg grating laser and applications in fiber lasers as single and multiple frequency and -wavelength sources are shown. Gain flattening and clamping of erbium amplifiers is another important area for long-haul high-bit-rate and analog transmission systems. Finally, the interesting and unique application of the fiber Bragg grating as a Raman oscillator is shown.

The ninth and final chapter deals with measurements and testing of Bragg gratings. This includes basic measurements, properties of different types of gratings, and measurement parameters. Life testing and reliability aspects of Bragg gratings conclude the book.

References

1 Hill K. O., Fujii Y., Johnson D. C., and Kawasaki B. S. "Photosensitivity in optical waveguides: Application to reflection filter fabrication," *Appl. Phys. Lett.* **32**(10), 647 (1978).

2 Bures J., Lapiere J., and Pascale D., "Photosensitivity effect in optical fibres: A model for the growth of an interference filter," *Appl. Phys. Let.* **37**(10), 860 (1980).

3 Lam D. W. K. and Garside B. K., "Characterisation of single-mode optical fibre filters," *Appl. Opt.* **20**(3), 440 (1981).

4 Ohmori Y. and Sasaki Y., "Phase matched sum frequency generation in optical fibers," *Appl. Phys. Lett.* **39**, 466–468 (1981).

5 Fujii Y., Kawasaki B. S., Hill K. O., and Johnson D. C., "Sum frequency generation in optical fibers," *Opt. Lett.* **5**, 48–50 (1980).

6 Österberg U. and Margulis W., "Efficient second harmonic in an optical fiber," in Technical Digest of *XIV Internat. Quantum Electron. Conf.,* paper WBB1 (1986).

7 Stolen R. H. and Tom H. W. K., "Self-organized phase-matched harmonic generation in optical fibers," *Opt. Lett.* **12**, 585–587 (1987).

8 Farries M. C., Russell P. St. J., Fermann M. E., and Payne D. N., "Second harmonic generation in an optical fiber by self-written $\chi^{(2)}$ grating," *Electron. Lett.* **23**, 322–323 (1987).

9 Stone J., "Photorefractivity in GeO_2-doped silica fibres," *J. Appl. Phys.* **62(11)**, 4371 (1987).

10 Kashyap R., "Photo induced enhancement of second harmonic generation in optical fibers," *Topical Meeting on Nonlinear Guided Wave Phenomenon: Physics and Applications,* 1989, Technical Digest Series, Vol. 2, held on February 2–4, 1989, Houston (Optical Society of America, Washington, D.C. 1989), pp. 255–258.

11 Hand D. P. and Russell P. St. J., "Single mode fibre gratings written into a Sagnac loop using photosensitive fibre: transmission filters," *IOOC, Technical Digest,* pp. 21C3–4, Japan (1989).

12 Bures J., Lacroix S., and Lapiere J., "Bragg reflector induced by photosensitivity in an optical fibre: model of growth and frequency response," *Appl. Opt.* **21**(19) 3052 (1982).

13 Meltz G., Morey W. W., and Glenn W. H., "Formation of Bragg gratings in optical fibres by transverse holographic method," *Opt. Lett.* **14**(15), 823 (1989).

14 Kashyap R., Armitage J. R., Wyatt R., Davey S. T., and Williams D. L., "All-fibre narrowband reflection gratings at 1500 nm," *Electron. Lett.* **26**(11), 730 (1990).

15 Lemaire P., Atkins R. M., Mizrahi V., and Reed W. A., "High pressure H_2 loading as a technique for achieving ultrahigh UV photosensitivity and thermal sensitivity in GeO_2 doped optical fibres," *Electron. Lett.* **29**(13), 1191 (1993).

16 Myers R. A., Mukherjee N., and Brueck S. R. J., "Large second order nonlinearity in poled fused silica," *Opt. Lett.* **16**, 1732–1734 (1991).

17 Bergot M. V., Farries M. C., Fermann M. E., Li L., Poyntz-Wright L. J., Russell P. St. J., and Smithson A., *Opt. Lett.* **13**, 592–594 (1988).

18 Kashyap R., "Phase-matched second-harmonic generation in periodically poled optical fibers," *Appl. Phys. Lett.* **58**(12), 1233, 25 March 1991.

19 Kashyap R., Borgonjen E., and Campbell R. J., "Continuous wave seeded second-harmonic generation optical fibres: The enigma of second harmonic generation," *Proc. SPIE* **2044**, pp. 202–212 (1993).

20 Fujiwara T., Wong D., and Fleming S., "Large electro-optic modulation in a thermally poled germanosilicate fiber," *IEEE Photon. Technol. Lett.* **7**(10), 1177–1179 (1995).

21 Fujiwara T., Takahashi M., and Ikushima A. J., "Second harmonic generation in germanosilicate glass poled with ArF laser irradiation," *Appl. Phys. Lett.* **71**(8), 1032–1034 (1997).

22 Philipp H. R., "Silicon dioxide (SiO_2) glass," in *Handbook of Optical Constants of Solids* (E. D. Palik, Ed.), p. 749. Academic Press, London. 1985.

23 Lines M. E., "Ultra low loss glasses," *AT&T Bell Labs. Tech. Memo. TM 11535-850916-33TM* (1985).

24 Yeun M. J., "Ultraviolet absorption studies in germanium silicate glasses," *Appl Opt.* **21**(1), 136–140 (1982).

25 Keck D. B., Maurer R. D., and Shultz P. C., "On the ultimate lower limit of attenuation in glass optical waveguides," *Appl. Phys. Lett.* **22**, 307 (1973).

26 See, for example, *SPIE 1516*, and articles therein.

27 Georges T., Delevaque E., Monerie M., Lamouler P., and Bayon J. F., "Pair induced quenching in erbium doped silicate fibers," *IEEE Optical Amplifiers and Their Applications,* Technical Digest, **17**, 71 (1992).

28 Ladoucer F. and Love J. D., in *Silica-Based Channel Waveguides and Devices.* Chapman & Hall, London (1996).

29 Williams D. L., Ainslie B. J., Armitage J. R., Kashyap R., and Campbell R. J., "Enhanced UV photosensitivity in boron codoped germanosilicate fibres," *Electron Lett.* **29**, 1191 (1993).

30 Camlibel I., Pinnow D. A., and Dabby F. W., "Optical ageing characteristics of borosilicate clad fused silica core fiber optical waveguides." *Appl. Phys. Lett.* **26**(4), 1183–1185 (1992).

31 Bansal N. P. and Doremus R. H., "Handbook of glass properties," Academic Press, New York, (1978).

32 Smith D. Y., "Dispersion theory, sum rules and their application to the analysis of optical data," in *The Handbook of Optical Constants,* (E. P. Palik, Ed.), Chapter 3. Academic Press, New York (1985).

33 Malitson I. H., "Interspecimen comparison of the refractive index of fused silica," *J. Opt. Soc. Am.* **15**(10), 1205–1209 (1965).

34 Fleming J., "Dispersion in GeO_2–SiO_2 glasses," *Appl. Opt.* **23**(4), 4486 (1984).

35 Hand D. P. and Russel P. St. J., "Photoinduced refractive index changes in germanosilicate optical fibers," *Opt. Lett.* **15**(2), 102–104 (1990).

36 Data on fused quartz, Hareaus-Amersil Inc.